PHYSICAL REVIEW B VOLUME 52, NUMBER 8 15 AUGUST 1995-II

Coupling between electrons and acoustic phonons in semiconductor nanostructures

P. A. Knipp
Department of Physics and Computer Science, Christopher Newport University, Newport News, Virginia 23606-2998

T. L. Reinecke
Naval Research Laboratory, Washington, D.C. 20375-5347
(Received 24 April 1995)

We show that the coupling between electrons and acoustic phonons in semiconductor confined structures occurs via an interaction, which we call the "ripple mechanism," in addition to the usual deformation potential coupling. Coupling due to the ripple mechanism arises from the perturbation of the electron wave function by the motion of interfaces. In this work we provide a general derivation of this coupling mechanism and give detailed expressions for it that are valid for all nanostructure systems, including those with quasi-zero-, one-, and two-dimensional geometries. For the purposes of illustration, calculations of the electron scattering rates due to acoustic phonons are given here for semiconductor quantum dots in a variety of shapes, including spheres, cubes, and rectangular parallelepipeds. From these results it is found that scattering due to the ripple mechanism dominates that from the deformation potential for dot sizes less than $\sim$ 500 Å and that for smaller dot sizes the ripple mechanism contribution can be much larger than that from the deformation potential.

I. INTRODUCTION

Electron scattering by acoustic phonons plays a key role in the physics of semiconductor nanostructures and in their potential applications. Recently it has been of particular interest in the context of carrier relaxation in quantum dots. Acoustic-phonon scattering controls the relaxation of carriers to their band bottoms, which is necessary for efficient laser action, for optical modulation, and for other optical and transport phenomena. It has been suggested that these relaxation rates may be slowed in lower-dimensional systems, leading to decreased optical efficiency. In considering the optical efficiency of nanostructure systems it is important to have a quantitative understanding of the relative importance of confinement on intrinsic processes, such as electron-phonon scattering, as compared to extrinsic effects such as those from fabrication induced defects. Such extrinsic effects generally degrade efficiency, but can often be controlled by improved fabrication. Intrinsic effects such as electron-phonon scattering rates, on the other hand, represent fundamental physical properties of these lower-dimensional systems. In particular, it is important to understand whether acoustic phonon relaxation rates are significantly altered by confinement.

The role of confinement on electron-phonon scattering has been of considerable interest recently. Extensive work has been done in recent years on confinement in LO-phonon scattering.[1] Although acoustic-phonon emission rates are generally not as fast as the corresponding LO processes, the former processes are the only ones capable of electronic relaxation down to the ground state. Only recently have the effects of confinement on electron–acoustic-phonon scattering begun to be addressed.[2] In this context, the issue of a possible "phonon relaxation bottleneck" in dot structures has been of particular interest.[3] Bockelmann and Bastard[2] have made calculations of the effects of dimensionality on scattering rates by acoustic phonons and they have shown that in the case of quantum dots in the shape of parallelepipeds, these rates drop off dramatically for lateral sizes less than $\sim$100 nm. Benisty *et al.*[3] have used results like these in a model of carrier relaxation to argue that the optical efficiency of such dots should decrease greatly for these small sizes because the electrons would not thermalize on the time scale of nonradiative losses due, for example, to defects.

All of the work to date[2–4] on electron–acoustic-phonon scattering in nanostructures, however, has been based on the deformation potential coupling between electrons and the phonons.[5] In the present work we show that there is an additional coupling mechanism between electrons and acoustic phonons that is intrinsic to systems that have interfaces.[6] It arises when acoustic phonons cause the interfaces to move and to perturb the electron wave functions. In the present context we refer to this scattering as due to the "ripple mechanism." It is analogous to the interaction involved when photons scatter inelastically from acoustic phonons in the vicinity of a free surface[7] or when free electrons scatter from the free surface of liquid He.[8] We show that this mechanism gives contributions to carrier scattering rates in nanostructures that can greatly exceed those of the deformation potential at small sizes and thus can potentially give qualitatively different results for carrier relaxation.

In the present work we first give a full derivation of the coupling due to the ripple mechanism for semiconductor nanostructures within the effective mass approxi-

0163-1829/95/52(8)/5923(6)/$06.00

mation for the electrons and elastic theory for the acoustic phonons. We derive compact expressions for the total carrier-phonon interaction that are valid for all geometries including quasi-zero-dimensional, one-dimensional, and two-dimensional systems. In addition, expressions are obtained for the limiting cases for which the potential offsets become infinitely large, leading to complete confinement of the electron states, which requires special care in the case of the ripple mechanism. This latter situation is one that is often used in discussing the physics of semiconductor nanostructures.

In order to illustrate the effects of the ripple mechanism we present here calculations of the electron–acoustic-phonon scattering rates in quantum dots of varying sizes and shapes. These shapes include spheres, cubes, and rectangular parallelepipeds. To facilitate comparison with experimental work and also comparison with previous calculations,[2] the numerical results given here are for the system of unstrained $In_{0.47}Ga_{0.53}As$ surrounded by InP, which is of considerable current interest.[9] We find that in the case of quantum dots the ripple mechanism scattering dominates that from the deformation potential for sizes $\lesssim 500$ Å. It should be noted that this is the regime of sizes in which the separation of the electronically quantized states becomes a few meV or greater and thus this is the class of systems that is of interest for its optical properties. Such quantum dot systems involving a number of materials are currently being investigated actively. Examples include approximately spherical dots of CdSe and CuCl in glass matrices[10] and a wide variety of lithographically formed dot structures in III-V and other materials approximately in the shapes of squares and rectangular parallelepipeds.[9,11]

In these calculations for quantum dots we discuss the effects of wave-function penetration into the barrier material on the scattering rates. We also discuss the relative contribution of the LA- and TA-phonon branches to the ripple mechanism scattering rates. Previously we have made explicit calculations of acoustic phonons and of their scattering by electrons including the effects of confinement on the acoustic phonons[6] and we find that the effects of confinement on the acoustic phonons in these such nanostructures have only small effects on the scattering rates. Thus, for simplicity, in the present work we represent the acoustic phonons as plane waves, two branches of which are transverse (TA) and one branch of which is longitudinal (LA).

In Sec. II we give a general derivation of the ripple mechanism interaction between electrons and acoustic phonons for nanostructures of arbitrary shape and composition. In Sec. III we give results for carrier scattering in quantum dots having a number of shapes, due to both the ripple mechanism and the deformation potential. Some concluding remarks are given in Sec. IV.

II. FORMALISM

For nanostructure systems having a spatially dependent carrier mass, Schrödinger's equation in the effective mass approximation is written[12]

$$-\frac{\hbar^2}{2}\nabla\cdot\left[\frac{1}{m(\mathbf{r})}\nabla\psi\right]+V(\mathbf{r})\psi=E\psi, \tag{1}$$

where $V(\mathbf{r})$ and $m(\mathbf{r})$ are the potential energy and effective mass governing the electron wave function $\psi(\mathbf{r})$. We will often be interested in materials for which $V(\mathbf{r})$ and $m(\mathbf{r})$ are "piecewise uniform," i.e., have (different) uniform values through each of several regions, such as is the case for material 1 (the "nanostructure") embedded in material 2 (the "barrier"). Examples of such systems include quantum wells, quantum wires, quantum dots, and superlattices. In this case the wave function is continuous across the interface separating the media and has a continuous "velocity" component $m(\mathbf{r})^{-1}\partial\psi/\partial n$ normal to the interface. If, in addition, $V(\mathbf{r})$ is taken to be infinite everywhere outside the nanostructure, then $\psi(\mathbf{r})$ is completely confined to the interior and vanishes on the boundary.

Charge carriers couple with acoustic phonons via two mechanisms, the deformation potential (DP) and the ripple mechanism (RM). The matrix element for the DP coupling is $D\langle i|\nabla\cdot\mathbf{u}|f\rangle$, where $\mathbf{u}(\mathbf{r})$ is the (appropriately normalized) acoustic displacement field, D is the DP coupling constant (typically $1-10$ eV), i is the initial electronic state, and f is the final electronic state. Hence the DP couples charge carriers to LA phonons but not to TA phonons. In the case that the LA phonon displacements are taken to be plane waves (proportional to $\hat{\mathbf{q}}\exp i\mathbf{q}\cdot\mathbf{r}$), the DP matrix element $M(\mathbf{q})$ becomes the Fourier transform of the product of the initial $[\psi_i(\mathbf{r})]$ and final $[\psi_f^*(\mathbf{r})]$ carrier wave functions.

Carrier-phonon coupling via the RM interaction occurs because of the spatial dependence of both $V(\mathbf{r})$ and $m(\mathbf{r})$ in Eq. (1). We call these two terms in the interaction Hamiltonian the "potential" term and the "mass" term in the ripple mechanism. It is convenient to derive the matrix elements due to these effects separately.

A. Potential term

We calculate this term in the interaction Hamiltonian using a Taylor expansion of the potential for small acoustic displacements

$$\begin{aligned}H_{\rm int}^{\rm pot}&=V[\mathbf{r}+\mathbf{u}(\mathbf{r})]-V[\mathbf{r}]\\&\approx V(\mathbf{r})+\mathbf{u}(\mathbf{r})\cdot\nabla V(\mathbf{r})-V(\mathbf{r})\\&=\mathbf{u}(\mathbf{r})\cdot\nabla V(\mathbf{r}).\end{aligned} \tag{2}$$

The matrix elements then are

$$\langle i|H_{\rm int}^{\rm pot}|f\rangle=\int d^3r\,\psi_i(\mathbf{r})\psi_f^*(\mathbf{r})\mathbf{u}(\mathbf{r})\cdot\nabla V(\mathbf{r}). \tag{3}$$

In the case of a piecewise-uniform potential $V(\mathbf{r})$

$$\nabla V(\mathbf{r})=(\Delta V)\int_S dA\,\delta(\mathbf{r}-\mathbf{r}_A)\hat{\mathbf{n}}_A. \tag{4}$$

Here S is the interface between the inner and outer media, $\mathbf{r}_A$ is a position on this interface, $\hat{\mathbf{n}}_A$ is the outwardly pointing surface normal, and $\Delta V\equiv V_2-V_1$, where $V_{1(2)}$ is the value of the uniform potential inside (outside) the

nanostructure. Now the matrix element becomes

$$\langle i|H_{\rm int}^{\rm pot}|f\rangle = (\Delta V)\int_S dA\,\psi_i(A)\psi_f^*(A)\mathbf{u}_A\cdot\hat{\mathbf{n}}_A. \quad (5)$$

B. Mass term

We let $f(\mathbf{r})\equiv 1/m(\mathbf{r})$, which gives for the interaction from the first term on the left-side of Eq. (1)

$$\begin{aligned} H_{\rm int}^{\rm mass} &= -\frac{\hbar^2}{2}\{\nabla\cdot[f(\mathbf{r}+\mathbf{u})\nabla]-\nabla\cdot[f(\mathbf{r})\nabla]\} \\ &\approx -\frac{\hbar^2}{2}\nabla\cdot\{[\mathbf{u}(\mathbf{r})\cdot\nabla f]\,\nabla\}. \end{aligned} \quad (6)$$

For this case the matrix element becomes

$$\begin{aligned} \langle i|H_{\rm int}^{\rm mass}|f\rangle &= -\frac{\hbar^2}{2}\int d^3r\,\psi_i\nabla\cdot\left[(\mathbf{u}\cdot\nabla f)\nabla\right]\psi_f^* \\ &= \frac{\hbar^2}{2}\int d^3r(\nabla\psi_i\cdot\nabla\psi_f^*)\mathbf{u}\cdot\nabla f \end{aligned} \quad (7)$$

by using Green's first identity. In the case of piecewise-uniform $m(\mathbf{r})$, the normal derivatives of the wave functions are continuous across the interface only if divided by $m(\mathbf{r})$. Here we use $\nabla\psi_i\cdot\nabla\psi_f^* = \overline{\nabla}\psi_i\cdot\overline{\nabla}\psi_f^* + (\partial\psi_i/\partial n)(\partial\psi_f^*/\partial n)$, where $\partial/\partial n$ is a normal derivative and $\overline{\nabla}$ is a tangential gradient. Then

$$\begin{aligned} \langle i|H_{\rm int}^{\rm mass}|f\rangle = \frac{\hbar^2}{2}\int d^3r\Bigg[&(\overline{\nabla}\psi_i\cdot\overline{\nabla}\psi_f^*)\mathbf{u}\cdot\nabla f \\ &-\left(\frac{1}{m}\frac{\partial\psi_i}{\partial n}\right)\left(\frac{1}{m}\frac{\partial\psi_f^*}{\partial n}\right)\mathbf{u}\cdot\nabla m\Bigg]. \end{aligned} \quad (8)$$

By using formulas for ∇f and ∇m analogous to Eq. (4) we obtain

$$\begin{aligned} \langle i|H_{\rm int}^{\rm mass}|f\rangle = \frac{\hbar^2 m_1 - m_2}{2}\int_S dA\Bigg|&\frac{\left(\overline{\nabla}\psi_i\cdot\overline{\nabla}\psi_f^*\right)}{m_1 m_2} \\ &+\left(\frac{1}{m}\frac{\partial\psi_i}{\partial n}\right)\left(\frac{1}{m}\frac{\partial\psi_f^*}{\partial n}\right)\Bigg|\mathbf{u}_A\cdot\hat{\mathbf{n}}_A, \end{aligned} \quad (9)$$

where m_1 is the value of the effective mass inside the nanostructure and m_2 is the value outside. The quantities in parentheses in Eq. (9) are continuous across the interface and thus are well defined at $\mathbf{r}=\mathbf{r}_A$.

The electronic properties of nanostructures often are treated by taking the potential outside to become infinite. In this case ΔV diverges, thereby confining the carrier wave functions to the nanostructure interior, and the quantities $\psi(A)$ [and $\overline{\nabla}\psi(A)$] go to zero, making the expression in Eq. (5) indeterminate. However, careful analysis yields the well-defined limit for this case:

$$\langle i|H_{\rm int}^{\rm pot}|f\rangle = \frac{\hbar^2 m_2}{2m_1^2}\int_S dA\,\left(\frac{\partial\psi_i}{\partial n}\right)\Bigg|_A\left(\frac{\partial\psi_f^*}{\partial n}\right)\Bigg|_A\mathbf{u}_A\cdot\hat{\mathbf{n}}_A, \quad (10)$$

where the normal derivatives are evaluated *inside* the nanostructure. Adding Eq. (10) to the corresponding limiting form of Eq. (9) yields for this case

$$\langle i|H_{\rm int}^{\rm tot}|f\rangle = \frac{\hbar^2}{2m_1}\int_S dA\,\left(\frac{\partial\psi_i}{\partial n}\right)\Bigg|_A\left(\frac{\partial\psi_f^*}{\partial n}\right)\Bigg|_A\mathbf{u}_A\cdot\hat{\mathbf{n}}_A. \quad (11)$$

As expected, ΔV and m_2 do not appear in Eq. (11) for this case (of a diverging potential in medium 2).

III. SCATTERING RATES IN DOTS

In order to illustrate the effects of the RM interaction in carrier scattering, we present here the results of calculations of electron scattering rates from both the RM and the DP interaction for quantum dots with a number of shapes. These calculations are done for dots of unstrained $In_{0.47}Ga_{0.53}As$ in InP.[13] The scattering rates are calculated using Fermi's golden rule, which in the case of the single-phonon processes considered here yields

$$\Gamma = \frac{2\pi}{\hbar}\int d^3q\,|M(\mathbf{q})|^2\,\delta(E_i - E_f - \hbar vq). \quad (12)$$

Here $\mathbf{q}$ is the phonon wave vector, v is the longitudinal sound speed, and $M(\mathbf{q})$ is the matrix element for electronic scattering accompanied by the emission of a phonon. We take the final state to be the dot's ground state and the initial state to be one of the (possibly degenerate) first-excited states.

From conservation of energy for single-phonon emission the typical phonon wave vector q is found to be considerably larger than the typical inverse nanostructure-size a^{-1} and these relatively large phonon wave vectors lead to several interesting consequences. (i) The phonons' spatial dependence can be approximated well by plane waves. In previous work[6] we have incorporated fully the effects of confinement on the acoustic-phonon spectrum by the nanostructure and we have found that it has only small effects on the electronic scattering. This is because for these relatively short wavelengths the acoustic discontinuity at the interface does not cause significant changes in the acoustic-phonon energy or wave function. (ii) For the RM scattering, the phonon momentum must be almost parallel to the surface normal in order that the integrand in Eqs. (5) and (11) does not contain many oscillations. Hence the TA-phonon displacements give rise to only small rippling of the interface and accordingly we find that the TA-phonon emission rate is smaller than the LA-phonon emission rate by a factor on the order of $(qa)^{-2}$ ($\ll 1$). (iii) The scattering rates can be calculated analytically owing to simplifications that can be made to the integral in Eq. (12). These simplifications are outlined separately below for each dot shape. (iv) The dependence of the scattering rate on the dot size exhibits rapid oscillations for the dot shapes studied here. For the DP coupling these oscillations mirror the high-q oscillations in the matrix element $M(\mathbf{q})$, which for this case is a Fourier transform. For the RM coupling these oscillations are due to the alternate presence at the interface S of nodes and antinodes of the phonon displacement $\mathbf{u}$. We have found that in realistic systems,

slight deviations in shape from the models studied here will smooth out these oscillations. Additionally, these deviations in shape will effectively prevent coherent interference between the DP- and the RM-coupling matrix elements. (v) The overall magnitudes of the matrix elements and scattering rates for both the DP and the RM are relatively small because the electron's wavelength is much larger than that of the acoustic phonon.

A. Spherical dot of radius a

For simplicity we take the potential outside of the dot to be infinite. Then the wave functions are given straightforwardly by

$$\psi_{nlm}(r,\theta,\phi) = j_l\left(\frac{x_{nl}r}{a}\right) Y_l^m(\theta,\phi), \tag{13}$$

where n $(= 1, 2, ...)$ is the radial quantum number, l and m are angular quantum numbers, Y_l^m is a spherical harmonic, $j_l(x)$ is a spherical Bessel function, x_{nl} is the nth zero of $j_l(x)$. The corresponding electronic energies are

$$E_{nlm} = \frac{\hbar^2 x_{nl}^2}{2m_1 a^2}. \tag{14}$$

The quantum numbers (nlm) for the ground state are (100) and for the threefold-degenerate first-excited state (nl) equals (11) and m equals 0 or ± 1.

For this shape the DP scattering rate is

$$\frac{0.141(N+1)D^2 m_1^5 v^3 a^2 \sin^2(\frac{5.15\hbar}{m_1 v a})}{\rho\hbar^6}, \tag{15}$$

where N is the phonon occupation function, v is the longitudinal sound speed, and ρ is the mass density. The RM scattering rate is

$$\frac{6.15(N+1)\hbar^2 \sin^2(\frac{5.15\hbar}{m_1 v a})}{\rho m_1 v a^6}. \tag{16}$$

These scattering rates are shown in Fig. 1 as a function of the dot diameter $2a$. The DP scattering rate is larger for large dot sizes, the RM rate is larger for small sizes, and these two scattering rates are equal for the diameter $2a = 3.21\hbar/(Dm_1^3 v^2)^{1/4} \approx 56$ nm for $In_xGa_{1-x}As$. Note from Eqs. (15) and (16) that the ratio of RM scattering to DP scattering increases without bound as the dot diameter decreases below 56 nm. In these calculations we find it useful to rearrange the integral over acoustic plane waves in Eq. (12) into an integral over *spherical* waves (with scalar quantum numbers l, m, and q). In this way we see that owing to the high symmetry of the spherical dot shape only one (spherical) phonon mode participates in the scattering process, making simple the calculation of the scattering rate Γ.

B. Cubical dot of dimensions $2a \times 2a \times 2a$

For infinite potential barriers, the wave functions are given straightforwardly by $\psi_{n_x n_y n_z}(x,y,z) = \sin\frac{n_x \pi x}{2a} \sin\frac{n_y \pi y}{2a} \sin\frac{n_z \pi z}{2a}$, where n_x, n_y, n_z are positive integers, and the electronic energies are $E_{nlm} = \frac{\hbar^2\pi^2}{8m_1 a^2}(n_x^2 + n_y^2 + n_z^2)$. For the ground state $(n_x n_y n_z)$ equals (111) and for the threefold-degenerate first-excited state $(n_x n_y n_z)$ equals (211), (121), or (112).

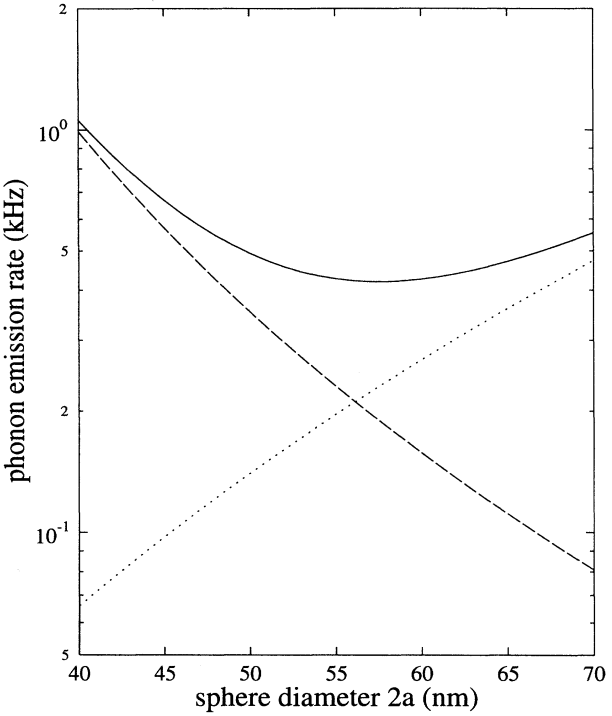

FIG. 1. Acoustic phonon emission rates for deformation potential scattering (dotted line) and ripple mechanism scattering (dashed line) for a spherical $In_xGa_{1-x}As$ dot in InP at $T = 300$ K. The solid line gives the total rate (Ref. 14).

The DP scattering rate is

$$\frac{0.42(N+1)D^2 m_1^5 v^3 a^2 \cos^2(\frac{3\pi^2\hbar}{8m_1 v a})}{\rho\hbar^6} \tag{17}$$

and the RM scattering rate is

$$\frac{40.1(N+1)\hbar^2 \cos^2(\frac{3\pi^2\hbar}{8m_1 v a})}{\rho m_1 v a^6}. \tag{18}$$

Thus the two rates are equal for the size $2a = 3.54\hbar/(Dm_1^3 v^2)^{1/4} \approx 62$ nm for $In_xGa_{1-x}As$ and the RM rate is considerably larger for smaller sizes. These results are qualitatively similar to those for the sphere, verifying the robustness of the conclusions given here about the importance of the ripple mechanism for small dot sizes. We find that the wave vectors of the phonon modes that participate in the scattering are predominantly oriented along one of the six equivalent cubical directions. This yields for the scattering rate Γ an integral over a spherical surface in $\mathbf{k}$ space whose integrand is peaked sharply for $\hat{\mathbf{k}}$ near these six different directions. Each of the resulting six integrals (which are added together) can be made dimensionless through a suitable change of variables and calculated straightforwardly.

C. Parallelepiped

For a dot of dimensions $2a \times 2a \times 2a_z$ surrounded by a material having an infinite band offset, the wave functions are $\psi_{n_x n_y n_z}(x,y,z) = \sin\frac{n_x \pi x}{2a} \sin\frac{n_y \pi y}{2a} \sin\frac{n_z \pi z}{2a_z}$ and the energies are $E_{nlm} = \frac{\hbar^2\pi^2}{8m_1}\left(\frac{n_x^2+n_y^2}{a^2} + \frac{n_z^2}{a_z^2}\right)$. Here we are interested in the case $a_z \ll a$, and a_z is often small enough that carrier tunneling in the z direction generally cannot be ignored, in which case the z part of the wave function and of the energy is altered in a straightforward fashion. For the ground state $(n_x n_y n_z)$ equals (111) and for the twofold-degenerate first-excited state $(n_x n_y n_z)$ equals either (211) or (121).

First we assume that the electron is not allowed to tunnel into the barrier. In this case the DP rate is

$$\frac{0.20(N+1)D^2 m_1^5 v^3 a^8}{\rho\hbar^6}\left[\frac{\sin q_z a_z}{a_z(a_z^2 - \frac{\pi^2}{q_z^2})}\right]^2, \tag{19}$$

where $q_z = 3\pi^2\hbar/(8m_1 v a^2)$. The RM rate is

$$\frac{0.617(N+1)\hbar^2 \sin^2 q_z a_z}{\rho m_1 v a_z^6}. \tag{20}$$

From Eqs. (19) and (20) the DP scattering rate is once again found to be larger for large a, the RM rate is larger for small a, and the rates are equal for $2a = 2.3\hbar/(Dm_1^3 v^2)^{1/4} \approx 40$ nm for $In_xGa_{1-x}As$.

If the electron is allowed to tunnel in the z direction, the result for the DP scattering expressed in Eq. (19) is modified by replacing the bracketed quantity with $\frac{q_z^3}{\pi^2}$ times the Fourier transform $M_z(q_z)$ in the z direction of the squared wave function. The result for the RM scattering in Eq. (20) is modified by replacing a_z^{-6} with $\left[\frac{8m_1\psi(a_z)^2\Delta V}{\hbar^2\pi^2}\right]^2$. We find that the ability of the electrons to tunnel out of a dot of thickness $2a_z = 5$ nm causes both the DP and the RM scattering rates to decrease by approximately two orders of magnitude from those given in Eqs. (19) and (20). This decrease can be explained simply based on the fact that both of these equations vary as a_z^{-6} (for large q_z), and a_z can be regarded as a measure of the vertical extent of the electron's wave function. For the present potential offset, allowing the electron to tunnel out of a 5-nm-thick dot amounts to increasing its vertical extent by approximately a factor 2, which when raised to the negative sixth power accounts for the roughly two orders of magnitude decrease in the scattering rates. The scattering rates (allowing for electron tunneling) are plotted in Fig. 2 for constant thickness $2a_z = 5$ nm and varying width $2a$. Note that the lateral size for which the DP rate and the RM rate are equal remains essentially unchanged from the above estimate, which was made based on the assumption that the electrons do not tunnel.

For the parallelepiped, we find that the wave vectors of the phonon modes that participate in the scattering are predominantly oriented along the z axis (as noted in Ref. 2 for the case of DP scattering). Hence the integrand for the scattering rate Γ is peaked sharply near $\hat{\mathbf{k}} = \pm\hat{\mathbf{z}}$ and the integral can be calculated straightforwardly as in the case for the cubical dot. The validity of the present results for the parallelepiped require that $a \gg a_z$ and that a is much greater than the phonon wavelength, but not necessarily that a_z greatly exceeds the phonon wavelength.

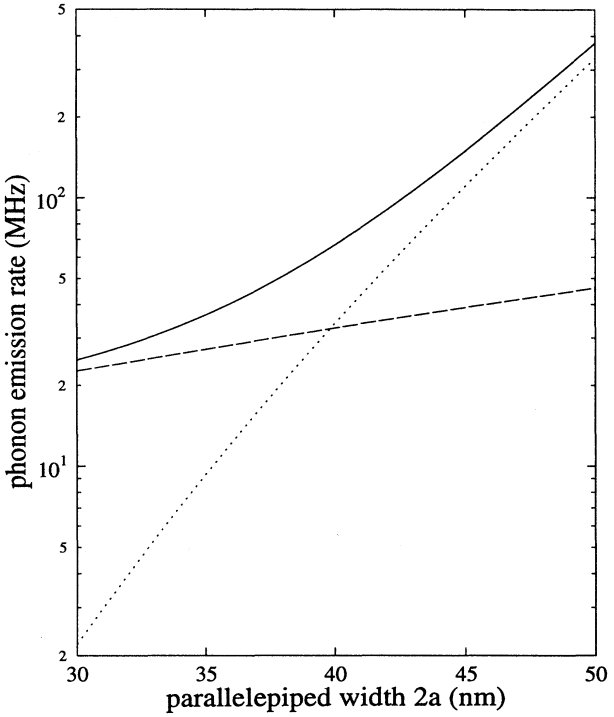

FIG. 2. Same as Fig. 1, but for $T = 300$ K and a dot shaped like a parallelepiped whose two widths are equal and whose thickness $2a_z$ is 5 nm (Ref. 14). The effects of wavefunction penetration into the barrier are taken into account as discussed in the text.

We have also studied scattering rates involving higher-lying electronic states in quantum dot systems. An example involves transitions for the rectangular parallelepiped from a state for which $(n_x, n_y, n_z) = (n, 2, 1)$ to a state for which $(n_x, n_y, n_z) = (n, 1, 1)$. This is a typical pair of states in the sense that the separation in energy between these two electronic states is comparable to the average energy spacing for the system, i.e., to the inverse of the density of states. In this case we find that both the DP and the RM scattering rates are independent of n as long as n is small enough so that the typical electronic momentum is essentially vertical (i.e., in the $\pm\hat{\mathbf{z}}$ direction). Thus the relative values of the DP and RM scattering rates are the same for these transitions as for those given above for the (121) $\rightarrow$ (111) transition.

IV. SUMMARY

In the present work we have shown that an interaction between electrons and acoustic phonons, which we call the ripple mechanism, is present in all semiconductor nanostructure systems in addition to the usual deforma-

tion potential coupling. We have given here a full derivation for the ripple mechanism valid for all nanostructure geometries, including quasi-zero-dimensional, one-dimensional, and two-dimensional systems.

In the present work we have illustrated the role of the ripple mechanism in electron scattering by calculating scattering rates for quantum dots of varying shapes and sizes including both the ripple mechanism and the deformation potential interaction. From these results, we have found that for dot sizes less than typically 50 nm the ripple mechanism gives scattering rates greater than those of the deformation potential coupling and that as the dot size becomes smaller the ripple mechanism scattering becomes orders of magnitude larger.

Acoustic-phonon scattering of carriers in quantum dots has attracted considerable attention recently because, based on the deformation potential scattering only, it has been argued that resulting relaxation rates of carriers in small quantum dots, of the range of sizes studied here, should be anomalously slow, leading to inefficient optical processes. The scattering rates calculated here are the appropriate inputs for a treatment of relaxation processes in such nanostructure systems. A full treatment of these relaxation rates is beyond the intent of the present work. From the present results, however, it is clear that an understanding of relaxation in quantum dots will require a treatment including the ripple mechanism scattering rates obtained here. Further, in light of the great difference for small dots between the ripple mechanism scattering rates and those from the deformation potential alone, it is possible that a treatment including these rates will give a qualitatively different picture of carrier relaxation in quantum dots than one based on the deformation potential alone.

The ripple mechanism scattering is expected to play an important role in the optical and transport properties of other nanostructures, including quantum wires and quantum wells. All of these systems have interfaces and will have contributions to carrier scattering from the ripple mechanism. For illustration here we have chosen to demonstrate this for the case of a quantum dot. Currently we are studying the effects of the ripple mechanism in quantum wires and quantum wells, where preliminary results indicate that this mechanism is not as important as the deformation potential.

Note added in proof. It has come to our attention that in recent work[15] Vasko and Mitin have discussed a particular example of what we call the ripple mechanism and have calculated the emission of TA phonons by the intrasubband scattering of electrons in a quantum well.

ACKNOWLEDGMENT

This work was supported in part by the U.S. Office of Naval Research.

[1] See, for example, M. V. Klein, IEEE J. Quantum Electron. **QE-22**, 1760 (1986); H. Rücker, E. Molinari, and P. Lugli, Phys. Rev. B **44**, 3463 (1991); P. A. Knipp and T. L. Reinecke, *ibid.* **48**, 5700 (1993), and references therein.

[2] U. Bockelmann and G. Bastard, Phys. Rev. B **42**, 8947 (1990).

[3] H. Benisty, C. M. Sotomayor-Torrès, and C. Weisbuch, Phys. Rev. B **44**, 10 945 (1991).

[4] M. A. Stroscio, K. W. Kin, SeGi Yu, and A. Ballato, J. Appl. Phys. **76**, 4670 (1994).

[5] The piezoelectric interaction with acoustic phonons is expected to be considerably weaker than the deformation potential interaction. See, for example, K. Hirakawa and H. Sakaki, Appl. Phys. Lett. **49**, 889 (1986); S. Rudin, T. L. Reinecke, and B. Segall, Phys. Rev. B **42**, 11 218 (1990).

[6] A preliminary version of the present work is given in P. A. Knipp and T. L. Reinecke, in *Proceedings of the 22nd International Conference on the Physics of Semiconductors*, edited by D. J. Lockwood (World Scientific, Singapore, 1995), p. 1927.

[7] A. M. Marvin, V. Bortolani, and F. Nizzoli, J. Phys. C **13**, 299 (1980).

[8] T. Martin, R. Bruinsma, and P. M. Platzman, Phys. Rev. B **38**, 2257 (1988).

[9] P. Ils, M. Michel, A. Forchel, I. Gyuro, M. Klenk, and E. Zielinski, Appl. Phys. Lett. **64**, 496 (1994), and references therein.

[10] See, e.g., T. Itoh, M. Nishijima, A. I. Ekimov, C. Gourdon, Al. L. Efros, and M. Rosen, Phys. Rev. Lett. **74**, 1645 (1995).

[11] See, e.g., Ch. Gréus, L. Butov, F. Daiminger, A. Forchel, P. A. Knipp, and T. L. Reinecke, Phys. Rev. B **47**, 7626 (1993).

[12] See, for example, G. Bastard, *Wave Mechanics Applied to Semiconductor Heterostructures* (Wiley, New York, 1988), Chap. III.

[13] For this system we use the following parameters: $m = 0.0434$, $v = 4300$ m/s, $\rho = 5.4$ g/cm^3, $D = 7.2$ eV, and a band offset of 200 meV.

[14] For purposes of plotting this figure the squared trigonometric function appearing in the formula for the scattering rate was replaced by its average value of 0.5. Also, the RM and the DP scattering rates were added incoherently to allow for the effects of slight deviations of shape.

[15] F. T. Vasko and V. V. Mitin, Phys. Rev. B **52**, 1500 (1995).